PHARMACIA

Pharmacia 70(3): 435–447
DOI 10.3897/pharmacia.70.e107041

Research Article

In silico study of the toxicity of hyperforin and its metabolites

Ivelin Iliev[1], Svetlana Georgieva[1], Yoana Sotirova[2], Velichka Andonova[2]

1 *Department of Pharmaceutical Chemistry, Faculty of Pharmacy, Medical University of Varna, Varna, Bulgaria*
2 *Department of Pharmaceutical Technologies, Faculty of Pharmacy, Medical University of Varna, Varna, Bulgaria*

Corresponding author: Ivelin Iliev (ivelin.iliev@mu-varna.bg)

Received 26 May 2023 ♦ **Accepted** 30 May 2023 ♦ **Published** 6 July 2023

Citation: Iliev I, Georgieva S, Sotirova Y, Andonova V (2023) *In silico* study of the toxicity of hyperforin and its metabolites. Pharmacia 70(3): 435–447. https://doi.org/10.3897/pharmacia.70.e107041

Abstract

St. John's wort is a medicinal herb well-known for its antidepressant, anti-inflammatory, antimycotic, and wound-healing properties. Hyperforin, the major phloroglucinol derivative, has been implicated as one of the main contributors to these therapeutic effects. Because of its high reactivity, this phytochemical can cause various adverse effects, such as allergic reactions, dizziness, dry mouth, and fatigue. To predict critical parameters of hyperforin's possible behavior after oral administration, *in silico* methods were applied. The pharmacokinetic profile, bioactivity, and toxicity of the phytochemical were analyzed by applying Molinspiration cheminformatics, SwissADME, PreADME/Tox, and OECD QSAR Toolbox software. The results showed adequate absorption, a high affinity for plasma proteins, and a prolonged renal excretion of the acylphloroglucinol. The high metabolic activity, a reason for potential cyto- and genotoxicity, and the predicted carcinogenicity and mutagenicity of hyperforin, necessitate further *in vitro* and *in vivo* tests.

Keywords

bioactivity, *Hypericum perforatum*, QSAR, metabolism, pharmacokinetics

Introduction

The application of St. John's wort (*Hypericum perforatum* L., Hypericaceae) dates back to ancient times: it has been known for treating wounds since Hippocrates and was used by Paracelsus for couping psychiatric disorders. (Mueller 1998; Barnes et al. 2001). Nowadays, controlled trials confirm this plant's efficacy in the treatment of mild to moderately severe depression. This therapeutic effect is mainly due to acylphloroglucinol hyperforin (Hyp). In terms of its mechanism of action, inhibition of neurotransmitters reuptake, such as dopamine, noradrenaline, and gammaaminobutyric acid, has been determined (Krusekopf and Roots 2005).

In addition to its antidepressive properties, Hyp possess other therapeutical effects, including anti-inflammatory activity through inhibition of the proliferation and induction of apoptosis of peripheral blood mononuclear cells (PBMC) (Krusekopf and Roots 2005); blocking of 5-LOX and COX-1, two crucial enzymes in the biosynthesis of pro-inflammatory eicosanoids (Albert et al. 2002); and significant relief of mild to moderate atopic dermatitis after topical application (Schempp et al. 2000).

The high reactivity of Hyp can lead to numerous side effects, such as allergic reactions, dizziness, dry mouth, fatigue, headache, restlessness, constipation, nausea, vomiting, and photosensitivity (Oyedepo and Palai 2021). Also, several studies have been published regarding Hyp as a potent inhibitor of CYP3A4 enzyme activity (Obach 2000; Lee et al. 2006) and a strong inducer of CYP3A4 expression (Moore et al. 2000; Komoroski et al. 2004; Madabushi et al. 2006). Despite its broad usage and

clinical importance, the metabolism of one of St. John's wort's pharmacologically most active components is not well characterized.

To address the question of its toxicity, we explored Hyp with *in silico* models. These complex mathematical algorithms facilitate an important task in chemistry and drug development: to predict the properties and biological activities of chemical compounds by their molecular structure (Berggren et al. 2017). Since non-animal methods are essential for the paradigm shift towards animal-free qualification of new compounds, the pharmaceutical industry is evolving alternative testing strategies and methodologies. Novel *in vitro* assays and *in silico* approaches have been developed for several toxicological endpoints, such as absorption, distribution, metabolism, excretion, and toxicity.

This study aims to analyze Hyp via *in silico* studies to expand the applications of the St. John's wort extracts previously obtained by the authors (Stefanov et al. 2022; Sotirova et al. 2023). To the best of our knowledge, there are no data on conducting such studies concerning this phytochemical's pharmacological properties, bioactivity, metabolism, and toxicity.

Materials and methods

To determine the metabolic activation, drug-likeness, bioactivity, and the pharmacokinetic and toxicological profile of Hyp *in silico*, the following freely-available software were used: Molinspiration Cheminformatics, SwissADME, PreADME/Tox and Organization for Economic Co-operation and Development (OECD) Quantitative structure-activity relationship (QSAR) Toolbox version 4.5.

Molinspiration cheminformatics, SwissADME, and PreADME/Tox software

For evaluation of the drug-likeness, bioactivity score, pharmacokinetic, and a brief toxicological profile *in silico*, the programs Molinspiration Cheminformatics (https://www.molinspiration.com/), SwissADME (http://www.swissadme.ch/index.php), and PreADME/Tox (https://preadmet.qsarhub.com/), were used. The structure of Hyp was analyzed in the modules for the prediction of molecular properties (Lipinski's rule of 5), bioactivity and absorption, distribution, metabolism, excretion (ADME), and toxicity. For the evaluation of each parameter, the following descriptors were chosen:

- properties–octanol-water partition coefficient (LogP; given as miLogP), total polar surface area (TPSA), molecular weight, number of H^- acceptors and donors, number of violations, number of rotatable bonds, and molecular volume;
- bioactivity–receptor and enzyme target prediction;
- absorption–absorption in Caco-2 cells and human intestinal absorption (HIA);
- distribution–plasma protein binding (PPB) and permeability in the blood-brain barrier (BBB);
- metabolism–interaction with enzymes from the Cytochrome P450 (CYP) complex;
- excretion–renal excretion through permeability in Madin-Darby canine kidney (MDCK) cells;
- toxicity–mutagenicity, carcinogenicity in rats and mice, and inhibition of the hERG gene.

Quantitative structure-activity relationship toolbox

For a more detailed evaluation of Hyp's toxicity, an OECD QSAR Toolbox software was used. The profiler '*In vivo* rat metabolism simulator' consists of 30–40 abiotic (non-enzymatic) and 630–640 enzyme-controlled reactions. The simulator also contains 520–530 enzymatic Phase I and 100–110 Phase II transformation reactions, but only metabolites (products) resulting from Phase I reactions are visualized. The 'Rat liver S9 metabolism' molecular transformations set comprise about 40–50 abiotic and a few enzyme-controlled reactions believed to occur at a very high rate. The simulator contains 450–460 enzymatic Phase I and 40–50 Phase II transformations. Only the generated *in vitro* metabolites (products) resulting from Phase I reactions are visualized. The principal applicability of these simulators is associated with the reproduction and prediction of the metabolic pathways of xenobiotics, which may elicit *in vivo* genotoxic effects (e.g., bacterial mutagenicity and chromosomal aberrations) (https://qsartoolbox.org/).

The profilers 'DNA binding by OASIS,' 'Protein binding by OASIS,' 'Toxic hazard classification by Cramer,' 'Carcinogenicity,' '*In vitro* mutagenicity,' and '*In vivo* mutagenicity' were used to elicit the toxicological profile of Hyp and its metabolites. The scope of 'DNA and Protein binding by OASIS' is to investigate the presence of alerts within target molecules that may interact with DNA and/or proteins (Mekenyan et al. 2004; Serafimova et al. 2007; https://qsartoolbox.org/). Categorization rules of chemicals into different levels (Class I (Low), II (Intermediate) and III (High)) of toxicological concern (when administered orally) are organized in a tree-like scheme in the 'Toxic hazard classification by Cramer' (https://qsartoolbox.org/). The 'Carcinogenicity' and '*In vitro* and *in vivo* mutagenicity' work as a decision tree for estimating carcinogenicity and *in vitro* (Ames test) and *in vivo* mutagenicity, based on a list of 55, 30, and 35 structural alerts, respectively (https://qsartoolbox.org/).

Results and discussion

Molecular properties and pharmacokinetic profile of Hyp

Determination of the molecular properties of Hyp was done using Molinspiration software. The results of the analysis are presented in Table 1.

Table 1. Pharmacokinetic parameters of hyperforin (Hyp) obtained using Molinspiration software.

Parameter	Result
miLogP	8.39
TPSA	71.44
Molecular weight	536.80
Number of H^- acceptors	4
Number of H^- donors	1
Violations	2
Number of rotatable bonds	11
Molecular Volume	559.15

Lipinski's rule of 5 states, 'The ideal drug molecule must have certain physicochemical properties.' and predicts if a biologically active molecule can be taken orally. According to this rule, a compound must have a molecular mass of less than 500 Da; LogP of less than 5; less than five hydrogen bond donors and ten hydrogen bond acceptors; polar surface area of 140 Å; and less than ten rotatable bonds (Lipinski 2004).

If a molecule does not infract more than one rule, it should have good pharmacokinetic properties and bioavailability in the organism. According to Lipinski's rule of 5, Hyp gives two violations, which make it less likely to be orally active. Nevertheless, one of the parameters, the molecular weight, is 7.2% higher than the limit–in this magnitude, it could not drastically affect the pharmacokinetics and bioavailability. In their scientific work, Biber et al. (1998) described the ranges of Hyp plasma levels after oral administration of St. John's wort alcoholic extracts. They have clarified that after oral administration, therapeutic doses can be achieved.

A more detailed pharmacokinetic analysis was made with PreADME/Tox software giving us information about the absorption, distribution, metabolism and excretion, and toxicity. Results are shown in Table 2.

Two main predictive models were analyzed to assess the absorption profile of Hyp: permeability in colon adenocarcinoma (Caco-2)-derived cells and the rate of human intestinal absorption (HIA). The obtained data showed excellent intestinal absorption (96.700160%) and medium cellular permeability after oral administration of Hyp.

To predict the distribution profile of Hyp, its ability to bind to plasma proteins and pass through the BBB was evaluated. The phloroglucinol derivative was found to have a high affinity for plasma proteins (100%) and high central nervous system (CNS) absorption (9.52384).

The metabolism of Hyp was assessed by its ability to inhibit four isoenzymes of the CYP450 complex—a family of liver enzymes responsible for the metabolism of endogenous substances and xenobiotics. The analyzed compound was found to be a CYP3A4 substrate and inhibitor (Obach 2000; Lee et al. 2006) and a CYP2C9 inhibitor. Compounds that are inhibitors of relevant isoenzymes should not be administered with other drugs or xenobiotics substrates of cytochrome P450 isoenzymes due to the risk of increased plasma concentrations or loss of effect.

Table 2. Pharmacokinetic and toxicological parameters of Hyp determined by PredADME/Tox software.

ADME/T Parameters	Result
Absorption	
HIA	96.700160
Caco-2	36.7417
Distribution	
PPB	100
BBB	9.52384
Metabolism	
CYP3A4	Substrate and Inhibitor
CYP2C19	–
CYP2C9	Inhibitor
CYP2D6	–
Renal excretion	
MDCK	51.9958
Toxicity	
P-glycoprotein	Inhibitor
Ames test	Non-mutagen
Carcinogenicity in rats	Positive
Carcinogenicity in mice	Positive
hERG Inhibition	Medium Risk

HIA: Low absorption 0.0–20.0%; moderate absorption 20.0–70.0%; excellent absorption 70.0–100.0% (Zhang et al. 2017);
Caco-2 cell permeability: High permeability > 70.0 $nm.sec^{-1}$; Medium permeability 4.0–70.0 $nm.sec^{-1}$; Low permeability < 4.0 $nm.sec^{-1}$ (Dolabela et al. 2018);
PPB: Strong connection: greater than 90.0%; weak connection: less than 90.0% (Zhang et al. 2017);
BBB: High CNS absorption: greater than 2.0; intermediate CNS absorption: between 0.1 and 2.0; low CNS absorption: less than 0.1 (Zhang et al. 2017);
MDCK: Low permeability: less than 25.0 $nm.sec^{-1}$; medium permeability: between 25.0 and 500.0 $nm.sec^{-1}$; high permeability: greater than 500.0 $nm.sec^{-1}$ (Zhang et al. 2017);
Ames test: Positive: mutagenic; Negative: non-mutagenic;
Carcinogenicity: Positive: carcinogenic; Negative: non-carcinogenic.

To analyze and predict the excretion profile of Hyp, the MDCK cell permeability model was evaluated. The phytochemical was found to have medium permeability to MDCK cells in this *in-silico* assay, suggesting that it would have a longer renal excretion time.

When assessing toxicity, the mutagenicity and carcinogenicity should also be analyzed. The model used for predicting the mutagenicity, the Ames test, confirmed that Hyp has a non-mutagenic effect. The *in silico* carcinogenicity prediction in rats and mice showed that the analyzed compound is a carcinogen. These results partially overlap with those obtained by the QSAR Toolbox software.

Another parameter in evaluating new drug compounds is cardiotoxicity. Inhibition of the hER gene leads to impaired expression of potassium channels and the subsequent occurrence of heart problems. In some cases, a fatal outcome is possible. Hyp was observed to have a medium risk in inhibiting the hER gene and, therefore, is not potentially cardiotoxic according to *in silico* tests.

In summary, Hyp has a good oral ADME profile according to the used PreADME/Tox software.

Drug-likeness and bioactivity

For evaluation of the drug-likeness, Molinspiration Cheminformatics and SwissADME software were used. Drug-likeness can be defined as a complex balance of different molecular properties and structural features that determine whether a given molecule is similar to a known drug. The variety of possible drug targets (each requiring a different combination of matching molecular features) is so vast that it is nearly impossible to test all *in vitro* or *in vivo*. This necessitates using *in silico* methods to predict the molecule's bioactivity. Results for bioactivity score from Molinspiration Cheminformatics software are presented in Table 3.

Table 3. Hyp bioactivity obtained using Molinspiration software.

Parameter	Result
GPCR Ligand	-0.10
Ion channel modulator	-0.20
Kinase inhibitor	-0.44
Nuclear receptor ligand	0.57
Protease inhibitor	-0.01
Enzyme inhibitor	0.25

As values less than 0 mean the molecule has no affinity for the corresponding target, it can be assumed that Hyp has an average affinity for nuclear receptors and a low affinity for enzymes.

The bioactivity of the acylphloroglucinol was determined in more detail with SwissADME software. Results for bioactivity score (Target Prediction) from SwissADME software are presented in Table 4.

Data showed that Hyp has activity towards various receptors and enzymes, explaining the high biological activity and the possibility of applying Hyp for multiple indications. The activity towards the nuclear Pregnane X receptor and the enzyme Prostaglandin E synthase was observed to be most significant, confirming the results obtained from Molinspiration software.

Quantitative structure-activity relationship

For evaluation of the metabolic activation and further toxicological analysis, the OECD QSAR Toolbox software was used. *In silico* study showed that Hyp cannot bind to DNA or proteins. However, according to the Toxic hazard classification by Cramer, Hyp is positioned in Class III. Due to alpha, beta-unsaturated carbonyl structural alert, it has carcinogenic and mutagenic (*in vitro* and *in vivo*) effects.

Applying a mathematical metabolism prediction model allowed us to identify and determine the metabolic activation of Hyp's structure. The resulting metabolites were also analyzed for their ability to bind to DNA and proteins, Toxic hazard classification by Cramer, carcinogenicity, and *in vitro* and *in vivo* mutagenicity.

In vivo rat metabolism simulator

As a result of the mathematical prediction performed using the *in vivo* rat metabolism simulator for Hyp, 103 metabolites were obtained, presented in Appendix 1: Table A1. In the scientific work of Hokkanen et al. (2011), it was found that Hyp gives 57 metabolites formed by monohydroxylation, hydroxylation, dehydrogenation, or a combination of these reactions.

DNA and protein binding

The wide range of possible metabolites predisposes to more pronounced pharmacological and/or toxic effects, necessitating the use of profilers such as the 'DNA and Protein binding by OASIS.' The ability of Hyp's resulting metabolites to bind to DNA and proteins is presented in Tables 5, 6, respectively.

Based on the analysis, Hyp probably can form metabolites that bind to DNA and proteins. The formers may induce genotoxicity, while the latter can directly affect the cell: by disrupting its primary functions or leading to damage indirectly.

Table 4. Hyp Swiss Target Prediction obtained using SwissADME software.

Target	Common name	Target class	Probability
Pregnane X receptor	NR1I2	Nuclear receptor	0.445899888539
Prostaglandin E synthase	PTGES	Enzyme	0.358235777561
Leukocyte adhesion glycoprotein LFA-1 alpha	ITGAL	Adhesion	0.0956237870388
Cytochrome P450 19A1	CYP19A1	Cytochrome P450	0.0956237870388
Arachidonate 5- lipoxygenase	ALOX5	Oxidoreductase	0.0956237870388
Type-1 angiotensin II receptor	AGTR1	Family A G proteincoupled receptor	0.0956237870388
Matrix metalloproteinase 13	MMP13	Protease	0.0956237870388
Matrix metalloproteinase 1	MMP1	Protease	0.0956237870388
Nitric oxide synthase, inducible	NOS2	Enzyme	0.0956237870388
Cyclooxygenase-2	PTGS2	Oxidoreductase	0.0956237870388
Endothelin receptor ET-A	EDNRA	Family A G proteincoupled receptor	0.0956237870388
Mineralocorticoid receptor	NR3C2	Nuclear receptor	0.0956237870388
11-beta-hydroxysteroid dehydrogenase 2	HSD11B2	Enzyme	0.0956237870388
Cholecystokinin B receptor	CCKBR	Family A G proteincoupled receptor	0.0956237870388
Angiotensin II receptor	AGTR2	Family A G proteincoupled receptor	0.0956237870388
Prostaglandin E synthase 2	PTGES2	Enzyme	0.0956237870388

Table 5. Binding of Hyp predicted metabolites to DNA.

Metabolite No.	Structural alert	Mechanistic alert	Mechanistic domain
1–10, 14, 16–18, 21–25, 27, 28, 31–36, 40, 41, 43–46, 49–52, 54, 56, 58–66, 68–81, 83–103	No alert found	–	–
55, 57, 67, 82	Alpha, betaunsaturated aldehydes	Schiff base formation	A_N^2
55, 57, 67, 82	Alpha, betaunsaturated aldehydes	Nucleophilic addition to alpha, beta- unsaturated carbonyl compounds	A_N^2
11–13, 15, 19, 20, 26, 29, 30, 37–39, 42, 47, 48, 53	Epoxides, aziridines, thiiranes, and oxetanes	Alkylation, directacting epoxides, and related	S_N^2

Table 6. Binding of Hyp predicted metabolites to proteins.

Metabolite No.	Structural alert	Mechanistic alert	Mechanistic domain
1–10, 16–18, 21–25, 27, 31–36, 40, 43–46, 49–52, 54, 56, 58–60, 62–66, 68–81, 83–91, 93–103	No alert found	–	–
55, 57, 61, 67, 82, 92	Aldehydes	Schiff base formation with carbonyl compounds	Schiff base formation
55, 57, 67, 82	Alpha, betaaldehydes	Michael's addition on alpha, beta-unsaturated carbonyl compounds	Michael addition
14, 28, 41	Ketones	Addition to carbon hetero-double bond	Nucleophilic addition
11–13, 15, 19, 20, 26, 29, 30, 37–39, 42, 47, 48, 53	Epoxides, aziridines, and sulfuranes	Ring-opening S_N^2 reaction	S_N^2

Toxic hazard classification by Cramer

The predicted metabolites were classified using the 'Toxic hazard classification by Cramer,' as shown in Table 7. The original Cramer decision tree consists of 33 questions, each answered ‚yes' or ‚no', leading to another question or the final classification into one of the three classes (I, II, and III) as follows (Cramer et al. 1978):

- Class I – Substances with simple chemical structures and for which efficient modes of metabolism exist, suggesting a low order of oral toxicity;
- Class II – Substances that possess structures that are less innocuous than class I substances but do not contain structural features suggestive of toxicity like those substances in class III;
- Class III – Substances with chemical structures that permit no strong initial presumption of safety or may even suggest significant toxicity or have reactive functional groups.

The parent structure Hyp is classified as Class III by the Toxic hazard classification by Cramer. Of the 103 generated metabolites, only one is classified as Class II, and all others belong to Class III. Even though there is no literature evidence, the results obtained by *in silico* studies indicated high oral toxicity of Hyp and its metabolites. In their study, Simona et al. (2016) described the influence of ethylene diammonium salt of Hyp on the morphology of internal organs and biochemical parameters. They classified it as Class V toxic—virtually non-toxic.

Table 7. Toxic hazard classification by Cramer of Hyp predicted metabolites.

Toxic hazard classification by Cramer	Metabolite No.
Class III	1–91, 93–103
Class II	92

Carcinogenicity and mutagenicity

Determination of carcinogenicity and mutagenicity is necessary for every drug molecule. The used software recognizes potential carcinogens (genotoxic and nongenotoxic) and mutagens (*in vitro* and *in vivo*) via one or more structural alerts embedded in their molecular structure. The results are presented in Table 8.

Seven structural alerts that can cause carcinogenicity were found among Hyp metabolites; for *in vitro* and *in vivo* mutagenicity, they were 3 and 4, respectively. However, all metabolites were found to have an alpha, beta-unsaturated carbonyl structural alert, which indicates a high probability of carcinogenic and *in vitro* and *in vivo* mutagenic effects.

In some scientific publications (Imreova et al. 2013, 2017; Peron et al. 2013), no carcinogenic or mutagenic effects have been established; thus, not all reactions in the organism are possible, which necessitates conducting *in vitro* tests such as that of Ames.

Rat liver S9 metabolism

As a result of the mathematical prediction performed using the Rat liver S9 metabolism simulator of Hyp, a total of 16 metabolites were obtained. They are presented in Appendix 1: Table A2.

DNA and protein binding

The wide range of possible metabolites predisposes to more pronounced pharmacological and/or toxic effects, necessitating the use of profilers such as DNA and protein binding by OASIS. The ability of Hyp's metabolites to bind to DNA and/or proteins is presented in Tables 9 and 10, respectively.

Table 8. Carcinogenicity (genotoxic and nongenotoxic) and mutagenicity (*in vitro* and *in vivo*) of Hyp predicted metabolites.

Structural alert	Carcinogenicity metabolite No.	*In vitro* mutagenicity metabolite No.	*In vivo* mutagenicity metabolite No.
Simple aldehyde	61, 92	61, 92	61, 92
Substituted n-alkylcarboxylic acid	25	–	–
Structural alerts for both genotoxic and nongenotoxic carcinogenicity	25	–	–
Structural alerts for nongenotoxic carcinogenicity	25	–	–
Epoxides and aziridines	11–13, 15, 19, 20, 26, 29, 30, 37–39, 42, 47, 48, 53	11–13, 15, 19, 20, 26, 29, 30, 37–39, 42, 47, 48, 53	11–13, 15, 19, 20, 26, 29, 30, 37–39, 42, 47, 48, 53
Structural alerts for genotoxic carcinogenicity	1–24, 26–103	–	–
Alpha, beta-unsaturated carbonyls	1–103	1–103	1–103
H-acceptor-path3-H-acceptor	–	–	1–103

Table 9. Binding of Hyp Rat liver S9 predicted metabolites to DNA.

Metabolite No.	Structural alert	Mechanistic alert	Mechanistic domain
1, 2, 4, 6, 8, 10–16	No alert found	–	–
3, 5, 7, 9	Epoxides, aziridines, thiiranes, and oxetanes	Alkylation, directacting epoxides, and related	S_N^2

Table 10. Binding of Hyp Rat liver S9 predicted metabolites to proteins.

Metabolite No.	Structural alert	Mechanistic alert	Mechanistic domain
1, 2, 4, 6, 8, 10–16	No alert found	–	–
3, 5, 7, 9	Epoxides, aziridines, and sulfuranes	Ring-opening S_N^2 reaction	S_N^2

Based on the analysis, it is believed that Hyp can form metabolites that can bind to DNA and proteins and, therefore, induce genotoxicity and/or cell damage.

Toxic hazard classification by Cramer

The predicted metabolites were grouped using the Toxic hazard classification by Cramer, as shown in Table 11. All of them are classified as Class III: these results suppose high oral toxicity of Hyp and his metabolites.

Carcinogenicity and mutagenicity

The results for carcinogenicity (genotoxic and nongenotoxic) and *in vitro* and *in vivo* mutagenicity are presented in Table 12.

Table 11. Toxic hazard classification by Cramer of Hyp predicted metabolites.

Toxic hazard classification by Cramer	Metabolite No.
Class III	1–16

Four structural alerts were found among Hyp metabolites: three causing carcinogenicity and three–mutagenicity (two and three for *in vitro* and *in vivo*, respectively). However, all metabolites were found to have an alpha, beta-unsaturated carbonyl structural alert, indicating a high probability of carcinogenic and *in vitro* and *in vivo* mutagenic effects.

Table 12. Carcinogenicity (genotoxic and nongenotoxic) and mutagenicity (*in vitro* and *in vivo*) of Hyp predicted metabolites.

Structural alert	Carcinogenicity metabolite No.	*In vitro* mutagenicity metabolite No.	*In vivo* mutagenicity metabolite No.
Epoxides and aziridines	3, 5, 7, 9	3, 5, 7, 9	3, 5, 7, 9
Structural alerts for genotoxic carcinogenicity	1–16	–	–
Alpha, beta-unsaturated carbonyls	1–16	1–16	1–16
H-acceptor-path3-H-acceptor	–	–	1–16

Conclusion

This study demonstrated sufficient absorption, high potential for plasma protein binding, high probability for crossing the blood-brain barrier, and a prolonged renal excretion of Hyp. The estimated ability of this acylphloroglucinol to alter certain CYP450 enzymes limits its coapplication with other active molecules due to possible drug interactions. Hyp also showed acceptable biological activity owing to the possibility of binding to various receptors and enzymes. The high metabolic activity of the phytochemical after oral administration and the ability of its metabolites to bind to DNA and/or proteins determine it as potentially geno- and cytotoxic. Cramer's decision tree classified Hyp and most of its metabolites as substances with reactive functional groups and no strong initial presumption of safety when administered orally. In addition, the phenolic derivative was predicted to have carcinogenic and mutagenic effects, which, however, are not supported by scientific literature. Thus, further investigations of Hyp's toxicity, carcinogenicity, and mutagenicity would benefit the research in phytochemistry and ethnopharmacology.

Acknowledgment

This work was funded by Fund "Nauka" at the Medical University of Varna, Bulgaria, through Project No. 18027, "Lipid

nanoparticles – a modern technological approach for inclusion of hyperforin with improved chemical stability in topical formulations for accelerated wound healing", Competition-Based Session for Scientific Research Projects, 2018.

References

Albert D, Zundorf I, Dingermann T, Muller WE, Steinhilber D, Werz O (2002) Hyperforin is a dual inhibitor of cyclooxygenase-1 and 5-lipoxygenase. Biochemical Pharmacology 64: 1767–1775. https://doi.org/10.1016/S0006-2952(02)01387-4

Barnes J, Anderson LA, Phillipson JD (2001) St. John's wort (*Hypericum perforatum* L): a review of its chemistry, pharmacology and clinical properties. Journal of Pharmacy and Pharmacology 53: 583–600. https://doi.org/10.1211/0022357011775910

Berggren E, White A, Ouedraogo G, Paini A, Richarz AN, Bois FY, Exner T, Leite S, Grunsven LAV, Worth A, Mahony C (2017) Ab initio chemical safety assessment: a workflow based on exposure considerations and non-animal methods, Computional Toxicology 4: 31–44. https://doi.org/10.1016/j.comtox.2017.10.001

Biber A, Fischer H, Römer A, Chatterjee SS (1998) Oral bioavailability of hyperforin from hypericum extracts in rats and human volunteers. Pharmacopsychiatry 31: 36–43. https://doi.org/10.1055/s-2007-979344

Cramer GM, Ford RA, Hall RL (1978) Estimation of toxic hazard – a decision tree approach. Food and Cosmetic Toxicology 16: 255–276. https://doi.org/10.1016/S0015-6264(76)80522-6

Dolabela MF, da Silva ARP, Ohashi LH, Bastos MLC, da Silva MCM, Vale VV (2018) Estudo *in silico* das atividades de triterpenos e iridoides isolados de *Himatanthus articulatus* (Vahl) Woodson. Revista Fitos 12(3): 227–242. https://doi.org/10.17648/2446-4775.2018.602

Hokkanen J, Tolonen A, Mattila S, Turpeinen M (2011) Metabolism of hyperforin, the active constituent of St. John's wort, in human liver microsomes. European Journal of Pharmaceutical Sciences 42: 273–284. https://doi.org/10.1016/j.ejps.2010.12.002

Imreová P, Miadoková E, Galová E, Chankova S, Chalupa I (2013) Potential anticlastogenic effect of hyperforin. Millitary Medical Science Letters (Vojenské Zdravotnické Listy) 82: 180–184. https://doi.org/10.31482/mmsl.2013.028

Imreova P, Feruszova J, Kyzek S, Bodnarova K, Zduriencikova M, Kozics K, Mucaji P, Galova E, Sevcovicova A, Miadokova E, Chalupa I (2017) Hyperforin exhibits antigenotoxic activity on human and bacterial cells. Molecules 22: e167. https://doi.org/10.3390/molecules22010167

Komoroski BJ, Zhang S, Cai H, Hutzler JM, Frye R, Tracy TS, Strom SC, Lehmann T, Ang CYW, Cui YY, Venkataramanan R (2004) Induction and inhibition of cytochromes P450 by the St. John's wort constituent hyperforin in human hepatocyte cultures. Drug Metabolism and Disposition 32(5): 512–518. https://doi.org/10.1124/dmd.32.5.512

Krusekopf S, Roots I (2005) St. John's wort and its constituent hyperforin concordantly regulate expression of genes encoding enzymes involved in basic cellular pathways. Pharmacogenetics and Genomics 15: 817–829. https://doi.org/10.1097/01.fpc.0000175597.60066.3d

Lee J-Y, Duke RK, Tran VH, Hook JM, Duke CC (2006) Hyperforin and its analogues inhibit CYP3A4 enzyme activity. Phytochemistry 67: 2550–2560. https://doi.org/10.1016/j.phytochem.2006.09.018

Lipinski CA (2004) Lead- and drug-like compounds: the rule-of-five revolution. Drug Discoveries Today: Technologies 1(4): 337–341. https://doi.org/10.1016/j.ddtec.2004.11.007

Madabushi R, Frank B, Drewelow B, Derendorf H, Butterweck V (2006) Hyperforin in St. John's wort drug interactions. European Journal of Clinical Pharmacology 62: 225–233. https://doi.org/10.1007/s00228-006-0096-0

Mekenyan O, Dimitrov S, Serafimova R, Thompson E, Kotov S, Dimitrova N, Walker J (2004) Identification of the structural requirements for mutagenicity by incorporating molecular flexibility and metabolic activation of chemicals I: TA100 model. Chemical Research in Toxicology 17: 753–766. https://doi.org/10.1021/tx030049t

Molinspiration Cheminformatics (1986) Molinspiration Cheminformatics. https://www.molinspiration.com/

Moore LB, Goodwin B, Jones SA, Wisely GB, Serabjit-Singh CJ, Willson TM, Collins JL, Kliewer SA (2000) St. John's wort induces hepatic drug metabolism through activation of the pregnane X receptor. Proceeding of the National Academy of Sciences of the Unated States of America 97: 7500–7502. https://doi.org/10.1073/pnas.130155097

Mueller BM (1998) St. John's Wort for depressive disorders: results of an outpatient study with the Hypericum preparation HYP 811. Advances in Therapy 15: 109–116.

Negreș S, Scutari C, Ionică FE, Gonciar V, Velescu B-Ș, Șeremet OC, Zanfirescu A, Zbârcea CE, Ștefănescu E, Ciobotaru E, Chiriță C (2016) Influence of hyperforin on the morphology of internal organs and biochemical parameters, in experimental model in mice. Romanian Journal of Morphology and Embryology 2: 663–673.

Obach RS (2000) Inhibition of human cytochrome P450 enzymes by constituents of St. John's wort, an herbal preparation used in the treatment of depression. Journal of Pharmacology and Experimental Therapeutics 294: 88–95.

Oyedepo TA, Palai S (2021) Herbal remedies, toxicity, and regulations. In: Egbuna C, Mishra AP, Goyal MR (Eds) Preparation of Phytopharmaceuticals for the Management of Disorders: The Development of Nutraceuticals and Traditional Medicine. Academic Press, Cambridge, Massachusetts, 89–127. https://doi.org/10.1016/B978-0-12-820284-5.00014-9

Peron AP, Mariucci RG, de Almeida IV, Düsman E (2013) Evaluation of the cytotoxicity, mutagenicity and antimutagenicity of a natural antidepressant, *Hypericum perforatum* L. (St. John's wort), on vegetal and animal test systems. BMC Complementary and Alternative Medicine 13: 1–97. https://doi.org/10.1186/1472-6882-13-97

PreADMET (2014–2023) PreADMET. https://preadmet.qsarhub.com/

QSAR Toolbox (2023) QSAR Toolbox. https://qsartoolbox.org/

Schempp CM, Winghofer B, Ludtke R, Simon-Haarhaus B, Schopf E, Simon JC (2000) Topical application of St John's wort (*Hypericum perforatum* L.) and of its metabolite hyperforin inhibits the allostimulatory capacity of epidermal cells. British Journal of Dermatology 142(5): 979–984. https://doi.org/10.1046/j.1365-2133.2000.03482.x

Serafimova R, Todorov M, Pavlov T, Kotov S, Jacob E, Aptula A, Mekenyan O (2007) Identification of the structural requirements for mutagenicity, by incorporating molecular flexibility and metabolic activation of chemicals. II. General Ames mutagenicity model. Chemical Research in Toxicology 20: 662–676. https://doi.org/10.1021/tx6003369

Sotirova Y, Gugleva V, Stoeva S, Kolev I, Nikolova R, Marudova M, Nikolova K, Kiselova-Kaneva Y, Hristova M, Andonova V (2023) Bigel formulations of nanoencapsulated St. John's wort extract–An approach for enhanced wound healing. Gels 9: e360. https://doi.org/10.3390/gels9050360

Stefanov S, Stoeva S, Georgieva S, Hristova M, Nikolova K, Dobreva M, Andonova V (2022) *In vivo* comparative assessment of incised wound healing in rats after application of hydrogel/organogel formulation containing St. John's wort methanol extract. Bulgarian Chemical Communications 54: 46–51. https://doi.org/10.34049/bcc.54.B2.0467

SwissADME (2023) Swiss Institute of Bioinformatics. http://www.swissadme.ch/index.php

Zhang S-N, Li X-Z, Yang X-Y (2017) Drug-likeness prediction of chemical constituents isolated from Chinese materia medica Ciwujia. Journal of Ethnopharmacology 198: 131–138. https://doi.org/10.1016/j.jep.2017.01.002

Appendix 1

Table A1. Numbers and structure of predicted metabolites of Hyp obtained by an *in vivo* rat metabolism simulator.

1.	2.	3.	4.
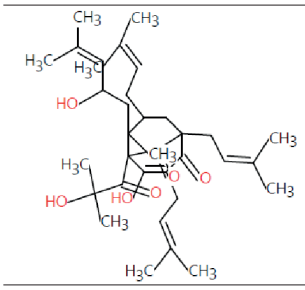	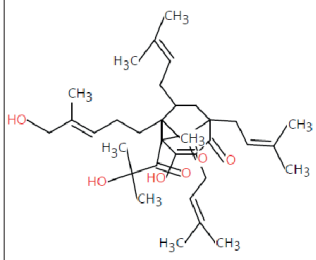	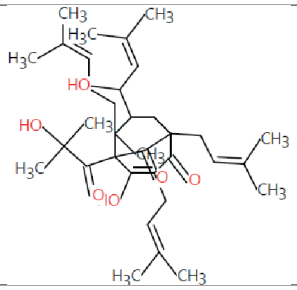	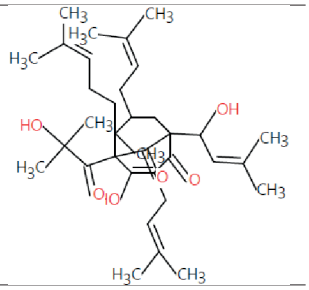
5.	**6.**	**7.**	**8.**
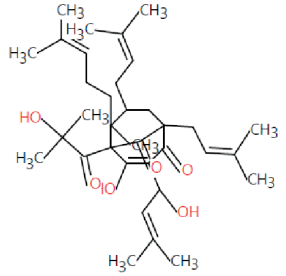	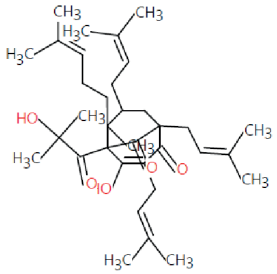	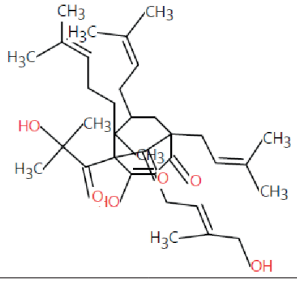	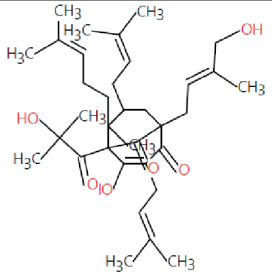
9.	**10.**	**11.**	**12.**
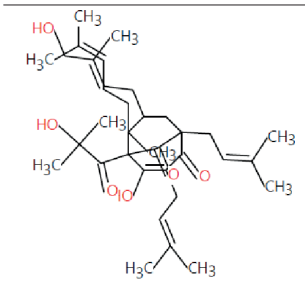	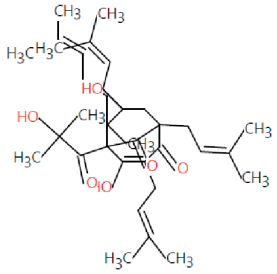	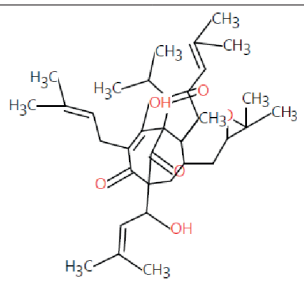	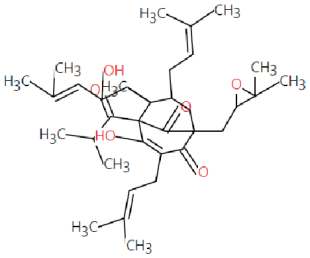
13.	**14.**	**15.**	**16.**
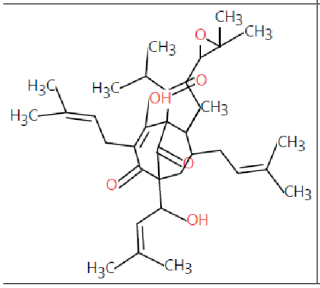	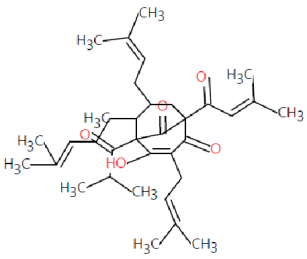	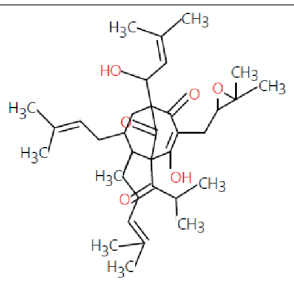	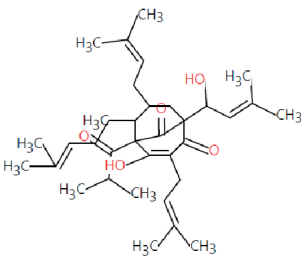

17.	18.	19.	20.
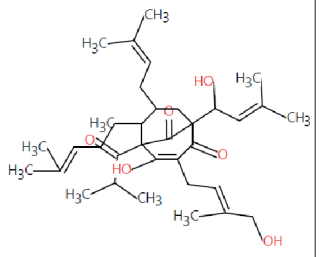	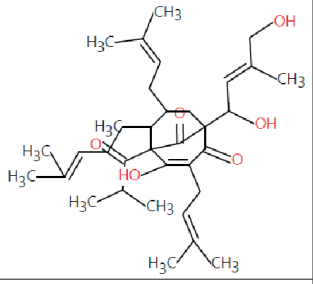	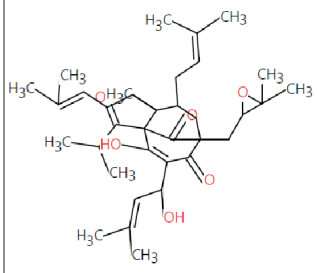	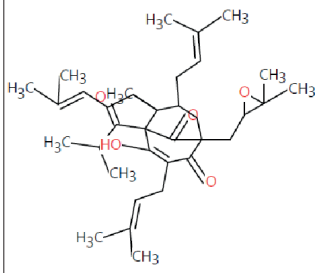
21.	22.	23.	24.
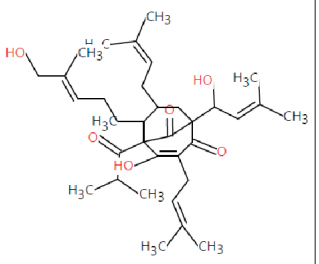	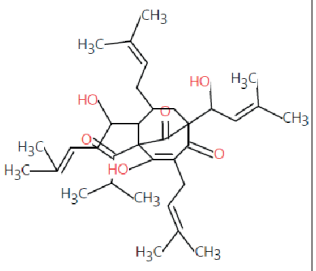	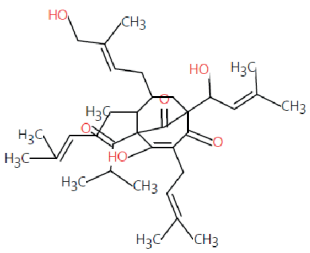	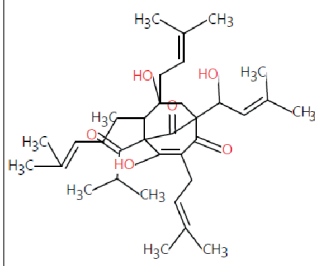
25.	26.	27.	28.
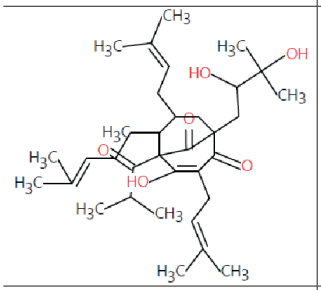	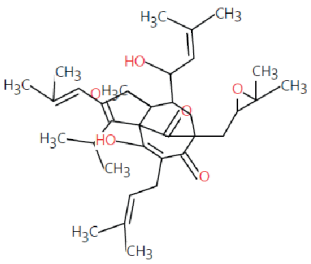	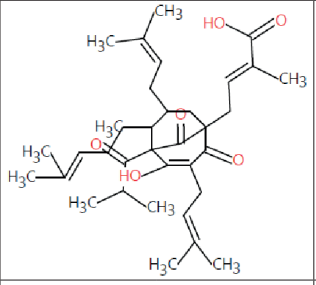	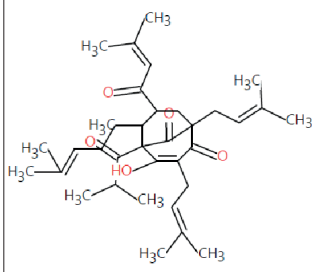
29.	30.	31.	32.
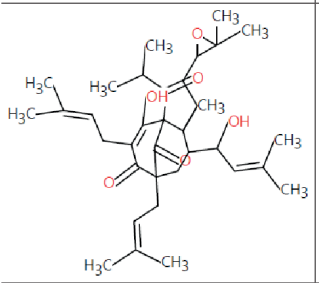	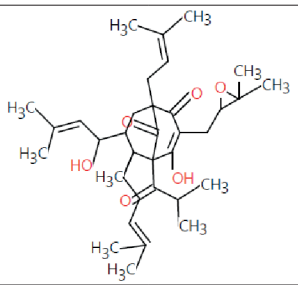	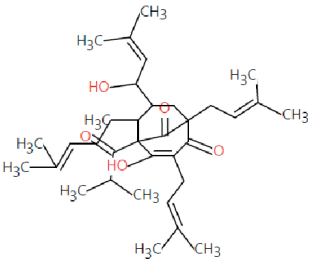	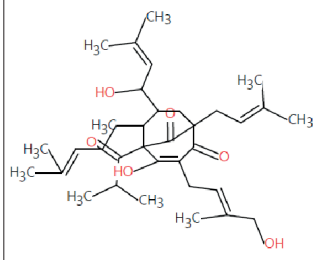
33.	34.	35.	36.
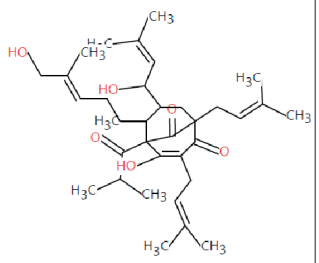	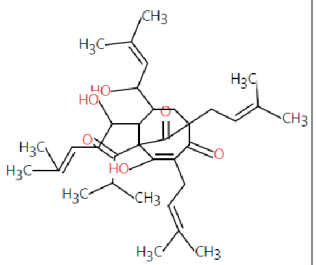	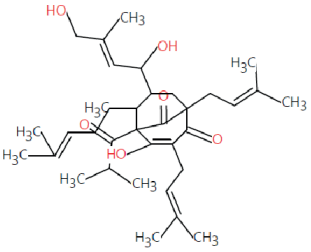	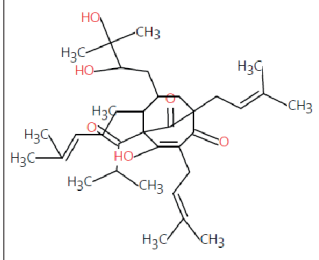
37.	38.	39.	40.
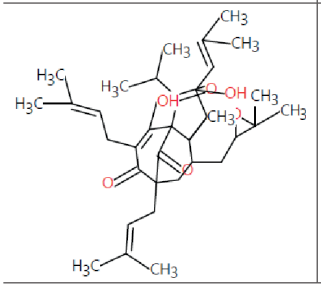	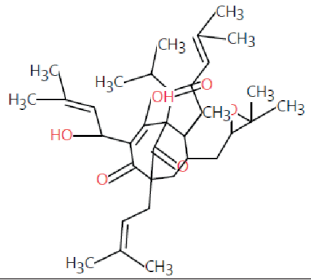	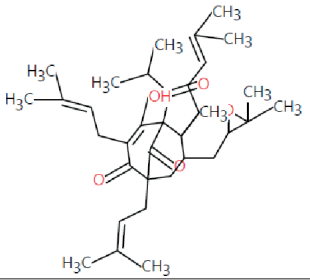	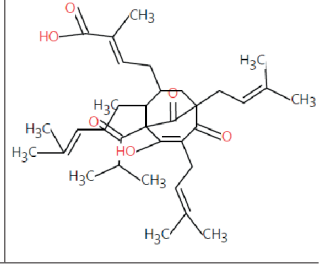

41.	42.	43.	44.
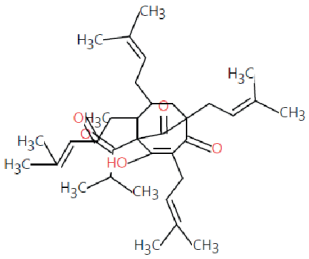	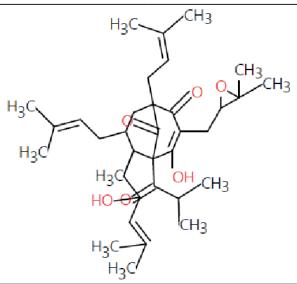	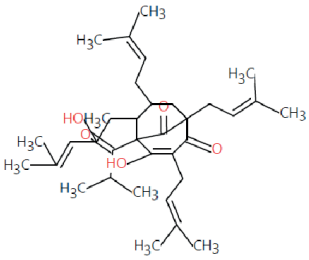	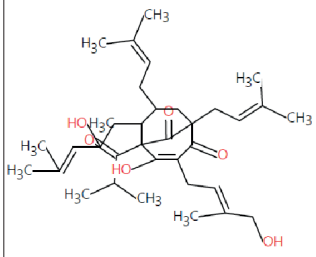
45.	46.	47.	48.
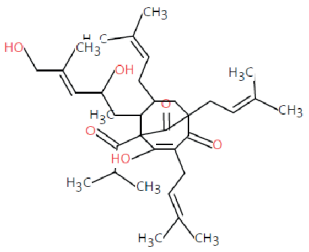	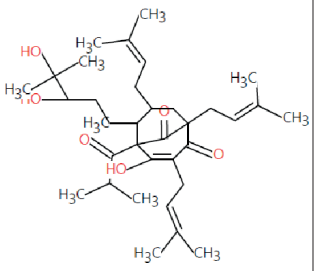	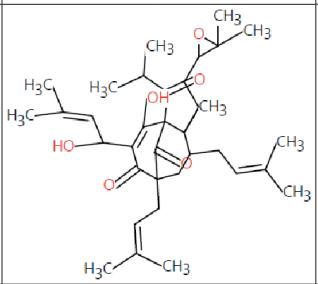	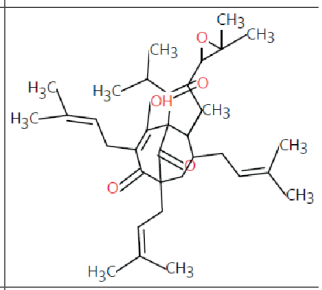
49.	50.	51.	52.
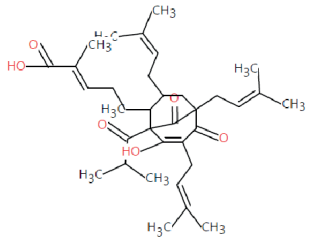	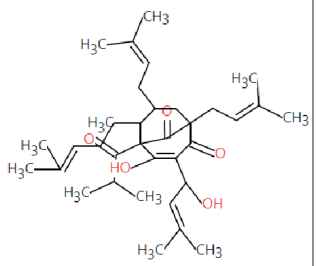	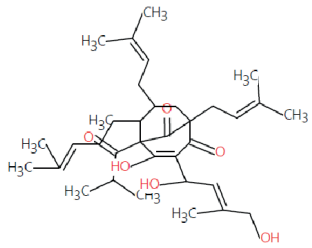	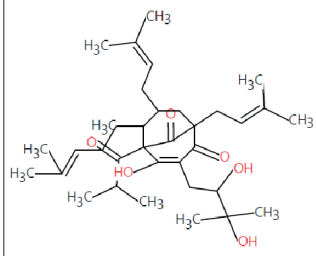
53.	54.	55.	56.
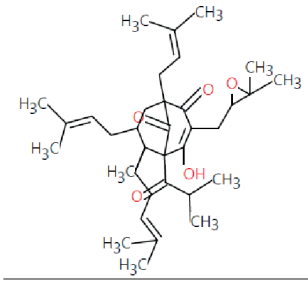	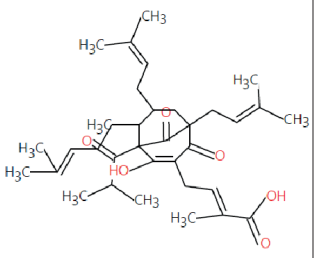	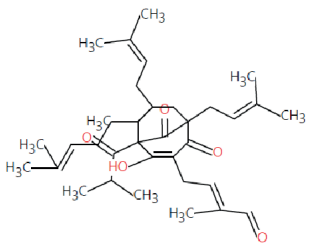	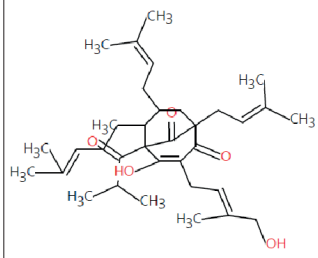
57.	58.	59.	60.
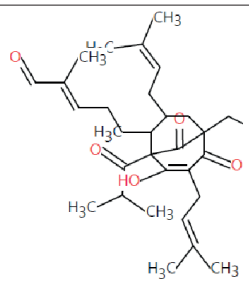	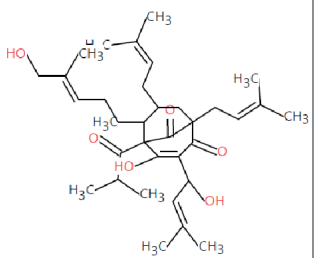	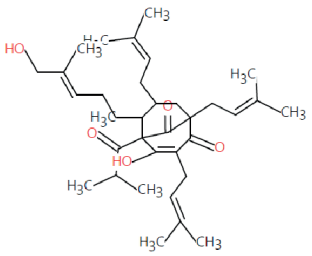	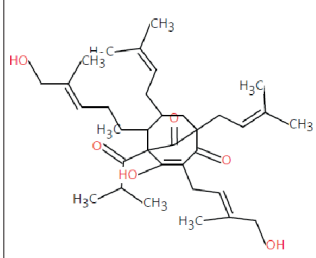
61.	62.	63.	64.
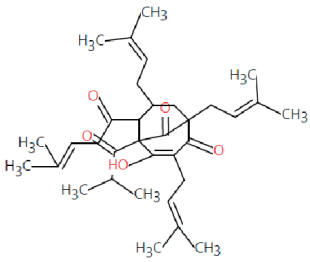	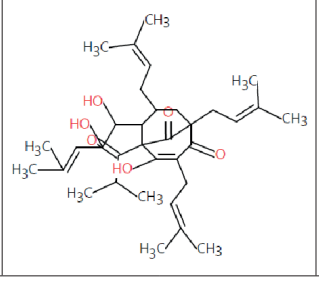	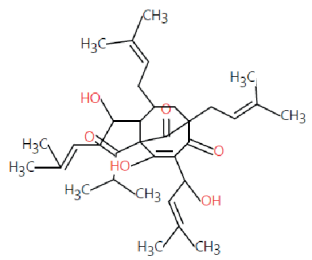	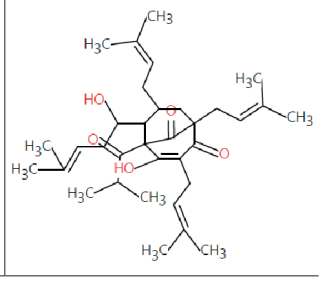

65.	66.	67.	68.
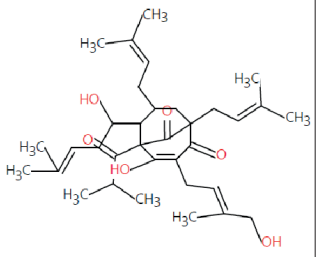	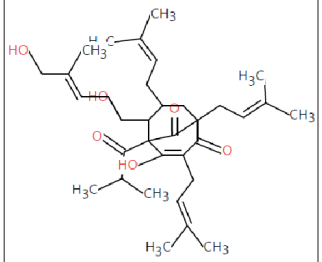	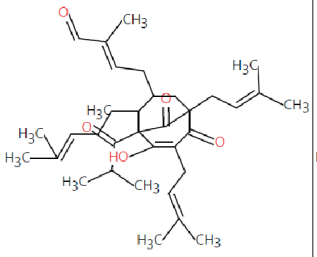	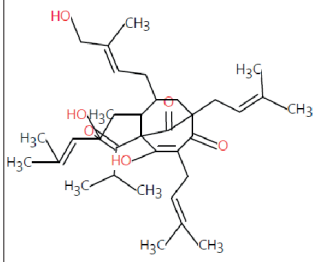
69.	70.	71.	72.
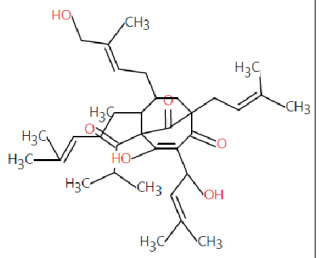	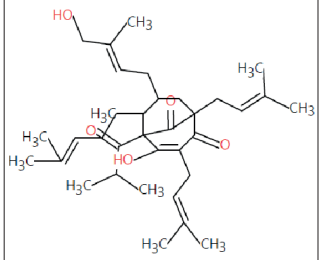	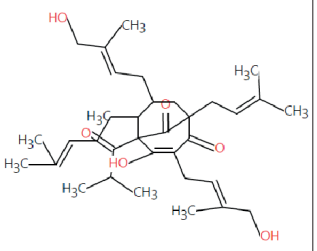	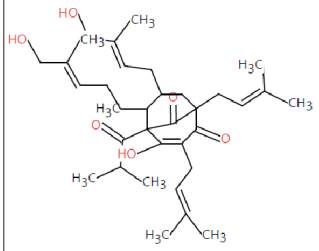
73.	74.	75.	76.
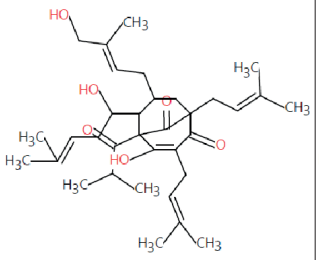	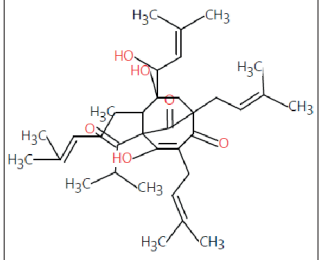	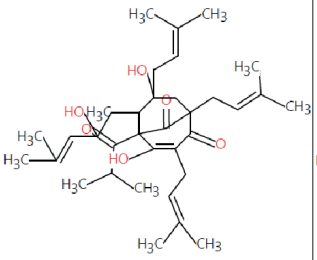	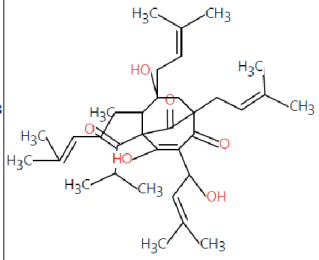
77.	78.	79.	80.
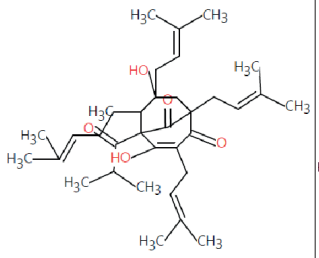	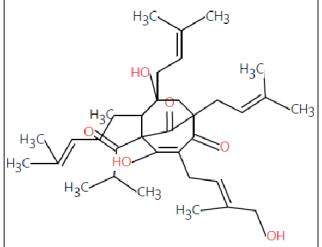	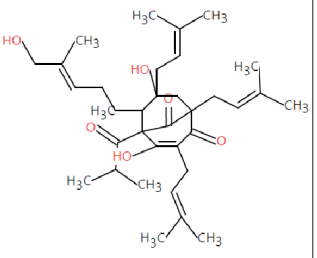	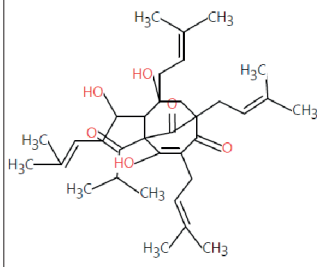
81.	82.	83.	84.
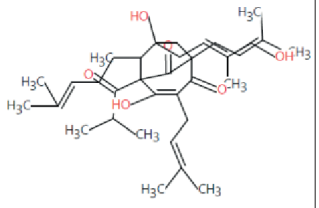	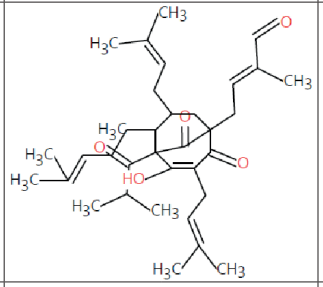	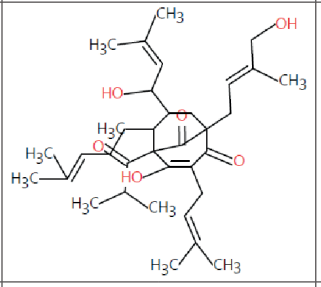	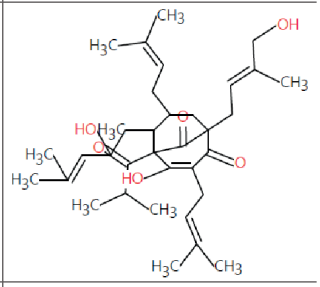
85.	86.	87.	88.
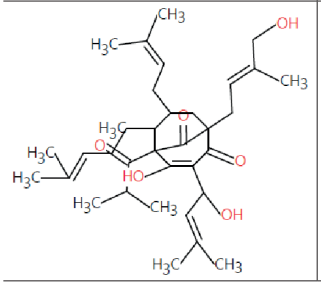	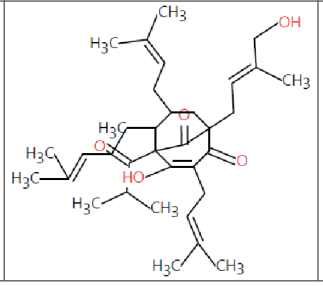	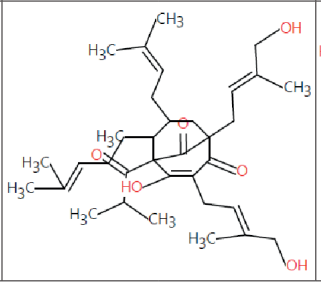	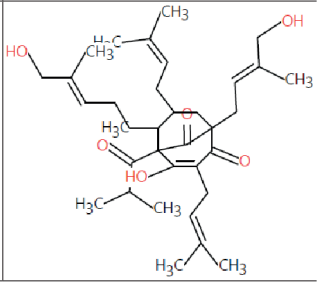

89.	90.	91.	92.
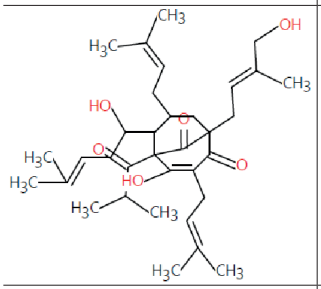	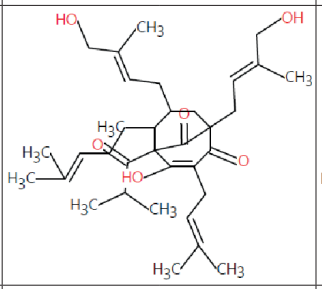	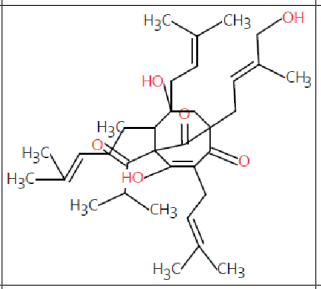	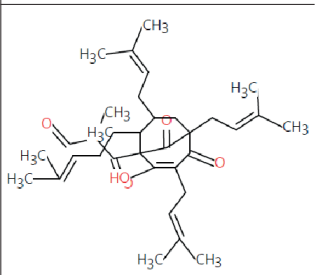
93.	**94.**	**95.**	**96.**
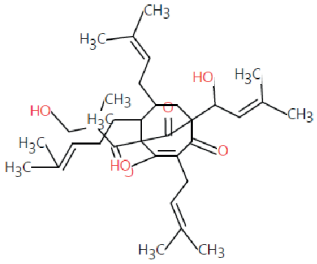	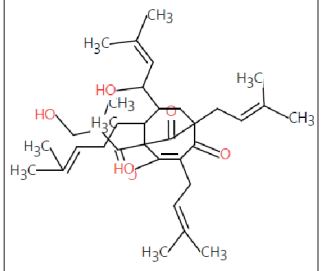	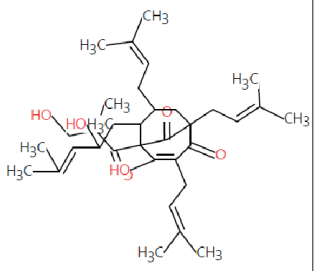	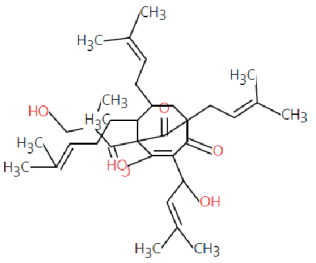
97.	**98.**	**99.**	**100.**
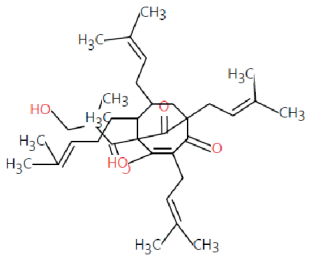	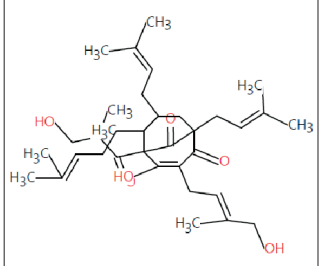	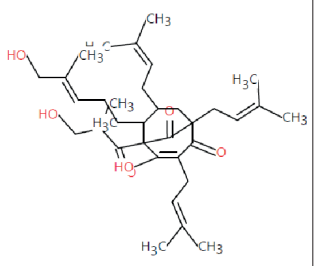	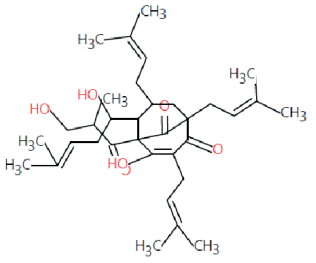
101.	**102.**	**103.**	
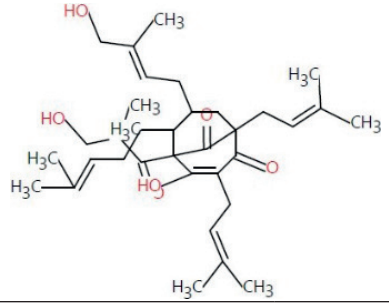	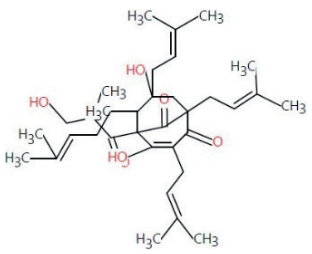	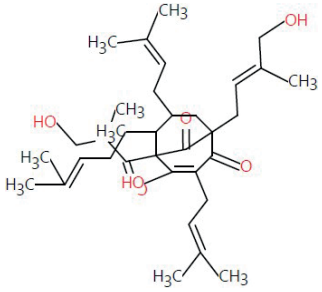	

Table A2. Numbers and structure of predicted metabolites of Hyp obtained by an *in vitro* rat metabolism simulator.

1.	2.	3.	4.
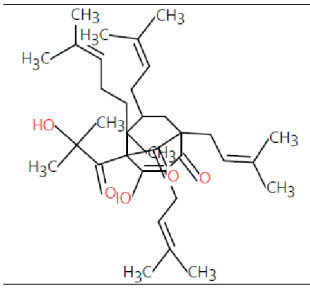	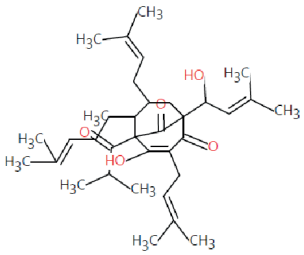	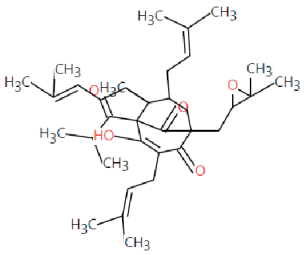	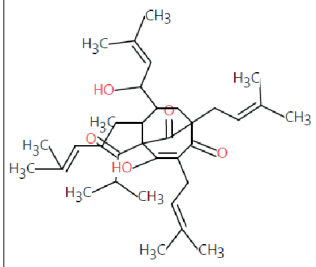
5.	6.	7.	8.
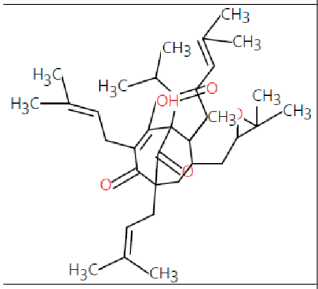	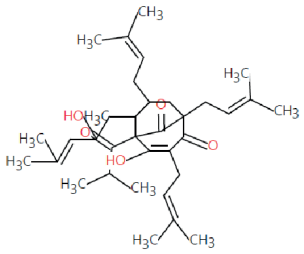	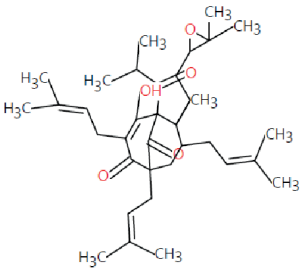	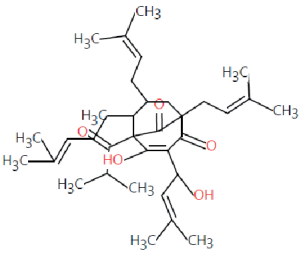
9.	10.	11.	12.
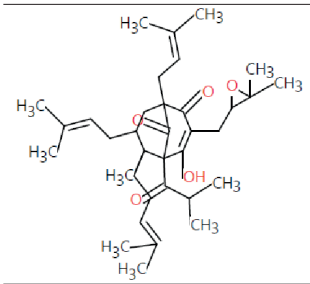	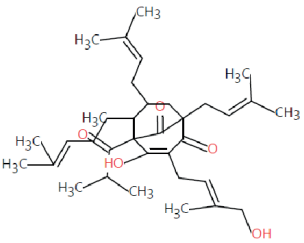	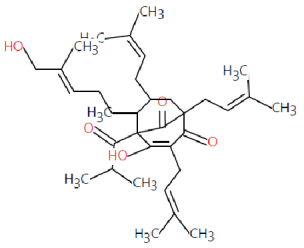	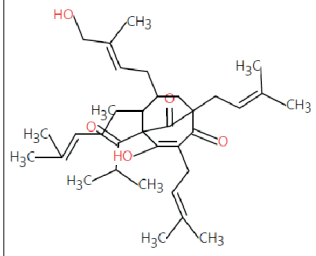
13.	14.	15.	16.